https://doi.org/10.5194/egusphere-2025-5466
Preprint. Discussion started: 21 November 2025

The potential of green infrastructure in urban pluvial flood mitigation - a scenario-based modelling study in Berlin

Sophia Dobkowitz[1], Leon Frederik De Vos[2], Deva Charan Jarajapu[1], Sarah Lindenlaub[1], Guilherme Samprogna Mohor[1], Omar Seleem[1], and Axel Bronstert[1]

[1]Institute of Environmental Science and Geography, University of Potsdam, Karl-Liebknecht-Str. 24-25, 14476 Potsdam, Germany
[2]Chair of Hydraulic Engineering, Technical University of Munich (TUM), Arcisstraße 21, 80333 München, Germany

Correspondence: Sophia Dobkowitz (sophia.dobkowitz@uni-potsdam.de)

Abstract. Urban surface sealing limits infiltration and thus increases the formation of runoff during heavy rain events. Green infrastructure (GI) measures can be used to reduce urban flood risk by promoting decentralized infiltration, water storage and evapotranspiration. With a scenario-based modelling study, we investigate the impact of green infrastructure on urban runoff formation, flood water depths and the resulting damage to buildings; comparing it with the impact of the conventional drainage system. The study area is located in the city of Berlin, in a heavily sealed 3.3 km^2 urban catchment. Design rain storms with a duration of one hour and totals between 15 and 100 mm are considered. The green infrastructure scenarios include different spatial extents and combinations of bioretention systems, green roofs and pervious pavement. The Storm Water Management Model is used for the urban runoff generation and the 2D-hydrodynamic module of TELEMAC for surface runoff concentration. Building damage is modelled with the Flood Damage Estimation Tool, a recursive partitioning tool developed with survey data representative of building damage caused by pluvial floods. Flood mitigation is investigated regarding absolute and relative reduction and also space efficiency of the GI types. Relative flood mitigation reduces at all modelling steps with increasing rain totals. In contrast, absolute runoff reduction increases with increasing rain totals while the area with maximum water level > 10 cm decreases the most at the 49 mm event and building damage reduces most at 25–30 mm. Bioretention systems achieve the highest spatial efficiency, however, green roofs and pervious pavements do not impede the former land use.

1 Introduction

Pluvial flooding is a ubiquitous risk in urban areas, as heavy surface sealing of urban environments inhibits infiltration and leads to increased and accelerated runoff concentration (Fletcher et al., 2013). Different from fluvial (riverine) flooding, urban pluvial flooding in this study refers to flood events in urban environments, mostly triggered by high-intensity convective rain events of small spatial extent and short duration, which surpass the capacity of the urban drainage system (Paprotny et al., 2021).

Negative pluvial flood impacts include damage to buildings, household goods and infrastructure, causing economic losses, temporally affected mobility and threats to human safety, including physical and psychological health (Berghäuser et al., 2021).

https://doi.org/10.5194/egusphere-2025-5466
Preprint. Discussion started: 21 November 2025

Overloaded and damaged sewer systems are further consequences of pluvial flooding from which problems for the environment and human health arise (Owolabi et al., 2022).

In many regions worldwide, an increase in frequency and intensity of heavy rain events has been observed and is expected to continue as a consequence of climate change (Caretta et al., 2022). As pluvial floods are triggered by heavy rain events, this also increases the hazard of pluvial floods.

The increase of heavy rain events can also be observed in Germany (Bürger et al., 2019, 2021). According to the heavy rainfall portal of the German Working Group on Water Issues of the Federal States and the Federal Government (LAWA Starkregenportal; LAWA, 2025), there were 13 events with return periods of 50 to over 100 years with the event maximum in Berlin in the period from 2002–2021. The longest of these events was the event of 2017-06-28 with a duration of 48 hours. With an area of 43 058 km^2 it had also clearly the largest spatial extent and with a rain total of 187.1 mm the highest event total. The remaining events had durations of 1–6 hours, with rain totals ranging from 44–109 mm and spatial extents of 15–514 km^2. The longest return period was attributed to the event of 2006-08-25 with a duration of 2 hours, rain total of 109 mm and a spatial extent of 44 km^2. Pluvial flood damages of residential buildings in Berlin during the same period (2002–2021) summed up to 174 million €, with 148 per 1000 residential buildings being affected (GDV, 2023).

Regarding water quality, also smaller rain events matter. The city centre of Berlin has a combined sewer system that conveys wastewater and stormwater together, which is very common in old European cities (Owolabi et al., 2022). When the capacity of the combined sewer system is overloaded due to heavy rainfall, combined sewer overflow (CSO) occurs. This means the release of untreated wastewater to the surface water bodies, deteriorating water quality (Owolabi et al., 2022; Weyrauch et al., 2010). Riechel et al. (2016) found that CSO happens about 30–40 times per year in Berlin, causing turbidity and low contents of dissolved oxygen in the river Spree. In the very sensitive areas of the city centre, rain events with more than 4.7 mm can already cause CSO (Riechel, 2009). Thus, pluvial flood mitigation measures should be effective across a wide range of rain intensities, covering extreme events, but also events of lower return periods.

Beginning in the 1980s, more holistic, multidisciplinary approaches to urban stormwater management have been developed, including several aspects beyond flood mitigation, such as recreation and aesthetics, water quality, stormwater as a resource and microclimate (Fletcher et al., 2015). Since then, several concepts were established in different regions, with different focuses but similar intentions. In this study, we use the term green infrastructure (GI) to refer to decentralized measures, with the aim of approaching the urban water cycle to a more natural state by increasing water retention, infiltration and evapotranspiration, which results in reduced surface runoff.

Riechel et al. (2020) showed that GI is an effective tool for CSO reduction. They investigated the impact of ambitious yet realistic GI scenarios in a study area located in Alt-Schöneberg, Berlin, that is with 70 % of impervious area heavily sealed. For an average rainfall year, the GI scenarios reduced total runoff by 28 %–39 % and peak runoff by 31 %–48 %. CSO volume even decreased by 45 %–58 %.

Neumann et al. (2024) estimated urban flood mitigation of various types, dimensions and implementation degrees of GI in a heavily sealed catchment in Berlin. Intensive green roofs and retention roofs turned out to provide very similar impact and

https://doi.org/10.5194/egusphere-2025-5466
Preprint. Discussion started: 21 November 2025

outperformed all other GI scenarios, resulting in a flood volume reduction of 33.5 % for the extreme rain event of 100 mm within 1 hour. CSO even decreased by 95 % for the same event.

Also in the centre of Berlin, Tügel et al. (2025) assessed the impact of retention roofs to mitigate urban flooding under current and future climate conditions. For the strongest rain event of 106.7 mm within 1 hour, the retention roofs reduced flood volume by 35 % and decreased CSO significantly but much less then reported by Neumann et al. (2024).

Both studies assessed the potential of GI for pluvial flood mitigation, however, the use of different measures of flood volume reduction complicates the comparison. While Tügel et al. (2025) used the sum of maximum water depth of all grid cells, Neumann et al. (2024) used only those cells with maximum water depth > 10 cm.

Despite the high costs caused by building damage from pluvial flooding, the above-mentioned studies did not include building damage. In order to address this research gap, we set up a multi-scenario analysis framework that integrates hydrological, hydrodynamic and building damage models to investigate the contribution of GI for pluvial flood mitigation in a heavily sealed catchment in the centre of Berlin, which is struggling with CSO.

In order to encourage reproduction and transfer to other study areas, this study is based on open source software (different from Neumann et al., 2024) and publicly available data (different from Tügel et al., 2025).

Our specific research questions are:

1. How much runoff retention can GI provide, compared to the conventional sewer system and the base scenario without any stormwater management?
2. How does the runoff retention propagate to flood water depth and building damage?
3. How do absolute and relative reduction of runoff, maximum water depth and building damage vary depending on the rain and retention scenarios?

In section 2, we will give an overview of the workflow and data, the study area, the rain and retention scenarios and the employed models and flood mitigation indices. In section 3, we will present the flood impact of the different rain and retention scenarios, considering different indices. In section 4, we will discuss the feasibility of the assessed retention scenarios, the benefit of space efficiency and compare our results to retention scenarios found in the literature. In section 5 we emphasize the outcome of our study for research and urban flood management.

2 Materials and methods

2.1 Workflow and data

The workflow of this study (Figure 1) is based on three different models, which are executed consecutively: Storm Water Management Model (SWMM; EPA, 2023) is used for the hydrologic modelling, TELEMAC-2D (EDF, 2022) for hydrodynamics and Flood Damage Estimation Tool (FlooDEsT; Samprogna Mohor et al., 2025) for the building damage estimation.

https://doi.org/10.5194/egusphere-2025-5466
Preprint. Discussion started: 21 November 2025

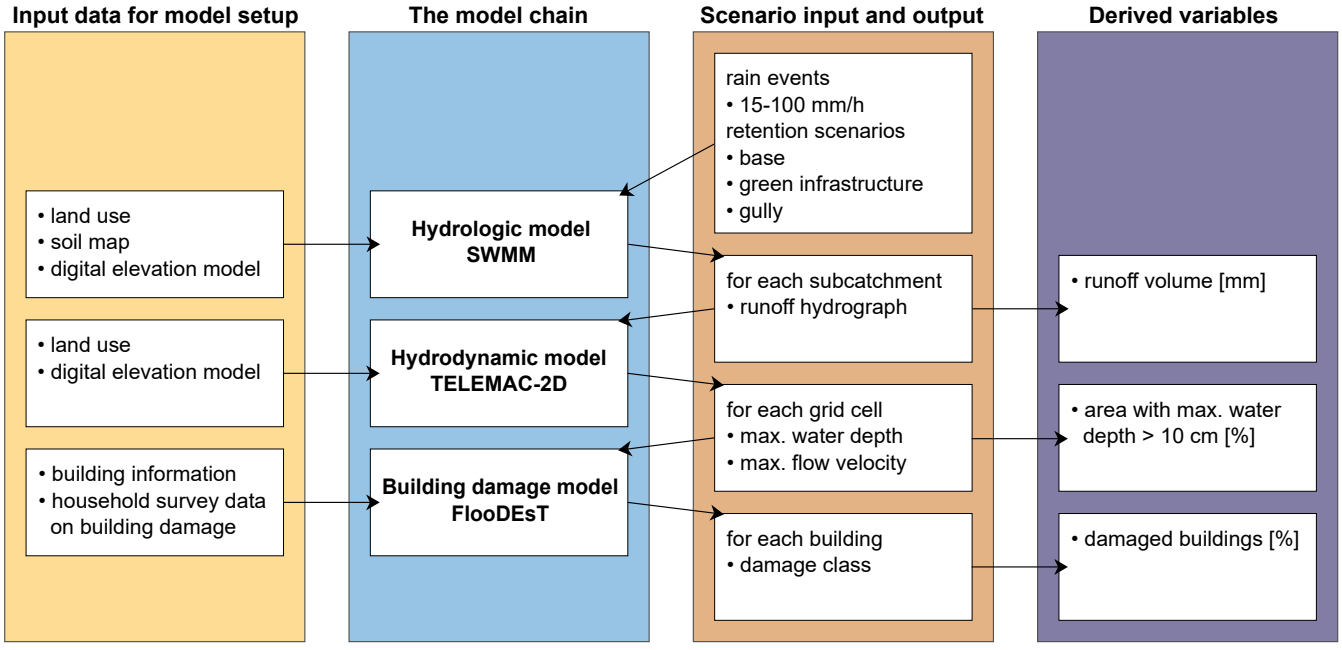

Figure 1. Workflow of data for model setup, scenario input and output through the model chain and derived variables.

These models require different input data. For the first two models, a land use map (vector shapefile; ALKIS, 2024) and a digital elevation model (DEM, 1 × 1 m; ATKIS, 2024) were used. SWMM additionally needs a soil map (250 × 250 m; ORNL DAAC, 2024). The training data for the model FlooDEsT result from household surveys on building damage caused by past pluvial flood events. In its application, FlooDEsT uses building information from cadastral data (OpenStreetMap contributors, 2024) as input. Additionally, missing building information is imputed from the existing survey data distributions.

For details on preprocessing of the input data, see section 2.4.

To start the model chain, a combination of a specific synthetic rain event and retention scenario is defined. This serves as input for SWMM, which then produces a runoff hydrograph for each subcatchment. This, in turn, is the scenario input for TELEMAC-2D, which spatially simulates maximum water depth and maximum flow velocity. These are used by FlooDEsT to model the damage class of each building.

2.2 Study area

The study area (Figure 2) is located in Berlin, i.e. in the district Friedrichshain-Kreuzberg/Mitte. With an area of 3.3 km^2 it is a small, very flat (heights in DEM ranging from 32–45 m a.s.l.) and highly sealed catchment, struggling with combined sewer overflows. The study area is defined by the sewage system subcatchment and is bounded by the river Spree in the northeast and by the canal Landwehrkanal in the south and east. 30 % of the catchment is covered by buildings, 25 % with roads and 9.2 % with parks, playgrounds and sports fields.

https://doi.org/10.5194/egusphere-2025-5466
Preprint. Discussion started: 21 November 2025

Table 1. Event total and maximum 5-min intensity of the investigated rain scenarios: KOSTRA events with return periods of 1-100 years and an additional extreme scenario, all with a duration of 1 hour and Euler-II temporal distribution.

Return period [years]	Event total [mm]	Max 5-min intensity [mm/h]
1	14.8	75.6
5	25.0	127.2
10	29.9	152.4
20	35.0	177.6
50	42.7	217.2
100	48.9	248.4
extreme	100.0	508.0

The climate in Berlin is classified according to the Köppen-Geiger classification as warm temperate with precipitation throughout the year and warm summers (Kottek et al., 2006). The mean annual precipitation (MAP) is 577.7 mm and monthly means range from 28.5 mm in April to 77.5 mm in July. The mean annual temperature is 10.4 °C, with monthly means ranging from 1.3 °C in January to 20.0 °C in July (DWD, 2023, weather station Berlin Mitte, reference period 1991–2020).

2.3 Scenario definition

2.3.1 Rainfall events

The German National Meteorological Service (DWD) provides, with KOSTRA 2020 (DWD, 2020a), a German-wide grid (5×5 km) of statistical heavy rain events with different durations (5 min to 7 days) and return periods (1–100 years), based on the period 1951–2020. Recently, the German Federal Agency for Cartography and Geodesy has released heavy rain maps for Berlin, using a simplified hydraulic methodology and two rainfall scenarios: an event with a return period of 100 years and an extreme event of 100 mm (BKG, 2025).

In order to cover a wide range of heavy rain intensities (Table 1), this study includes synthetic rain events with a duration of one hour, based on the KOSTRA 2020 return periods of 1, 5, 10, 20, 50 and 100 years. As the study area is located in KOSTRA tile number 105190, this corresponds to rain totals of 14.8–48.9 mm for the investigated return periods (DWD, 2020b). Additionally, as suggested by BKG (2025), an extreme event with a rain total of 100 mm was included.

The temporal resolution of the synthetic rain events is 5 min, following Euler-II distribution, as it is established in Germany for the design of drainage systems (DWA, 2021). For example, the 100-year event has a rain total of 48.9 mm, with the following 12 consecutive 5-min rain totals: 3.3, 4.5, 7.4, 20.7, 2.3, 2.3, 1.6, 1.6, 1.6, 1.2, 1.2 and 1.2 mm. The maximum 5-min intensity of the selected rain events ranges from 75.6 to 248.4 mm/h for the KOSTRA events, for the extreme event it is 508.0 mm/h.

https://doi.org/10.5194/egusphere-2025-5466
Preprint. Discussion started: 21 November 2025

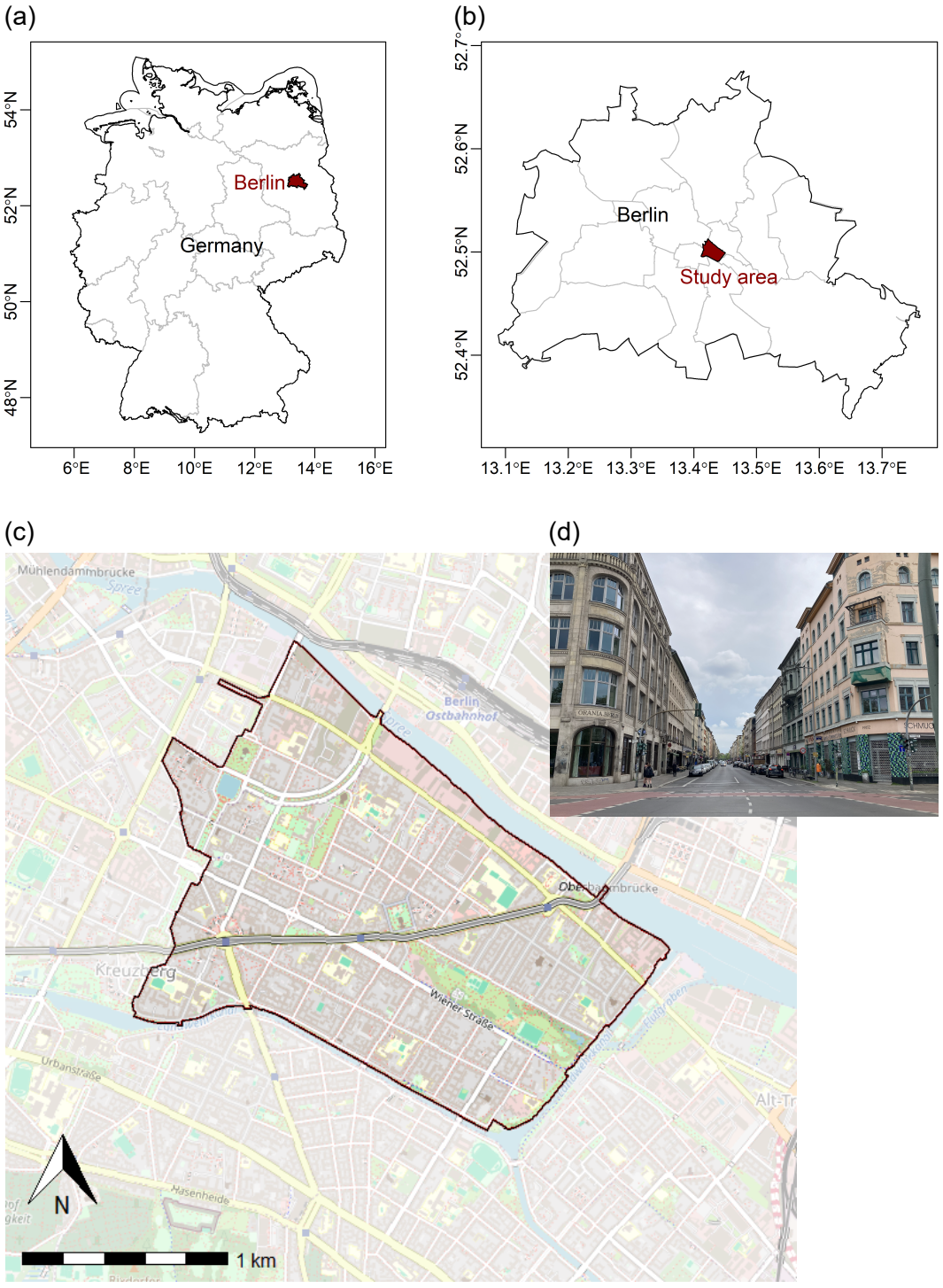

Figure 2. Study area location in Friedrichshain/Kreuzberg, Berlin: (a) Berlin in Germany; (b) location of the study area in Berlin; (c) land cover (© OpenStreetMap contributors, 2025, distribution under ODbL license); (d) typical street in the study area.

https://doi.org/10.5194/egusphere-2025-5466
Preprint. Discussion started: 21 November 2025

2.3.2 Conventional stormwater management

The conventional stormwater management scenario (hereafter "gully" scenario) is designed following the recommendations for drainage systems of DIN EN 752-2 (Sieker and Neidhart, 2018). Here, the capacity of drainage systems in urban or residential areas is designed to fully meet a precipitation event with a return period of 5 years. As our study area is located in the highly urbanised city centre of Berlin, we define gullies with a corresponding capacity of 16 mm in 15 min on all roads in the study area.

2.3.3 Green infrastructure

The assessed GI scenarios consist of single and combined GI measures, including three types of infiltration-based GI (see Dobkowitz et al. (2025) for more details on the GI measures):

- **Bioretention system (BR):** A shallow depression that collects surface runoff from surrounding impervious areas. The soil layer is covered with plants over a storage layer made of sand or gravel to obtain an elevated hydraulic conductivity. Optionally, at the bottom, there is an underdrain to the sewer system. BRs help to reduce runoff and remove pollutants.
- **Green roof (GR):** A greened soil layer over a drainage mat on top of a building, allowing the retention and evapotranspiration of water on roofs with inclinations of up to 45°. We can distinguish between extensive GR with a soil layer thickness of a few centimetres and intensive GR with a soil layer of at least 12 cm up to over a metre.
- **Pervious pavement (PP):** The pavement layer can be made of either impermeable paving blocks with permeable gaps filled with substrate, possibly with grass growing in them, or an asphalt layer which is porous itself. Below, there is a storage layer with an optional underdrain, like for the BR. PP can be used for roads, sidewalks, squares and car parks.

For the maximum GI scenarios, potential GI extents were defined as follows: BR on 10 % of the study area, after subtracting the area covered by buildings (BR_{max}), GR on all buildings (GR_{max}) and PP on 50 % of the roads (PP_{max}). Based on these definitions, the medium GI scenarios were defined as half of the maximum extents (BR_{med}, GR_{med} and PP_{med}).

Additionally, two combined scenarios were defined, GR_{max}+PP_{med} and BR_{max}+GR_{max}. For both of them, GR_{max} was combined with one of the other GI types because there is no spatial overlap between them.

Table 2 provides an overview of the retention scenario definitions and the respective percentage of the study area that is impervious, pervious or covered by GI. The base and gully scenarios include no GI, with an impervious area of 55.3 % and a pervious area of 44.7 %. For the GI scenarios, the GI area is subtracted from the impervious and/or pervious areas, resulting in impervious areas ranging from 20.0 % to 54.1 %, pervious areas of 40.4–44.7 % and GI areas of 3.4–36.0 %.

The GI types BR, GR and PP are implemented in SWMM as "LID Controls", i.e., "Bio-Retention Cell", "Green Roof" and "Permeable Pavement". For the required input parameters we extracted typical design parameters from the literature (Dobkowitz et al., 2025). As loamy sand is common in Berlin, we deduced the soil hydraulic parameters from this soil type. In addition, recommendations from the SWMM 5.2 User Guide (EPA, 2023) were followed, resulting in the set of parameters shown in Table 3.

https://doi.org/10.5194/egusphere-2025-5466
Preprint. Discussion started: 21 November 2025

Table 2. Retention scenarios: definition, impervious, pervious and green infrastructure (GI) covered areas.

Scenario	Definition	Impervious area [%]	Pervious area [%]	GI area [%]
base	no GI, no gully	55.3	44.7	0.0
gully	no GI, with gully	55.3	44.7	0.0
BR_{max}	10 % of the study area without buildings	52.9	40.4	6.8
BR_{med}	5 % of the study area without buildings	54.1	42.5	3.4
GR_{max}	100 % of the buildings	26.1	44.7	29.2
GR_{med}	50 % of the buildings	40.7	44.7	14.6
PP_{max}	50 % of the roads	43.1	44.7	12.2
PP_{med}	25 % of the roads	49.2	44.7	6.1
GR_{max}+PP_{med}		20.0	44.7	35.3
BR_{max}+GR_{max}		23.7	40.4	36.0

The unit area of a certain GI type is replicated within each subcatchment until reaching the defined spatial extent. In the case of GR and PP, the surface width per unit is used to define how the overland flow leaves the GI unit. For BR, instead, the surface width is zero as the runoff just spills over the berm. BR and PP receive all runoff from impervious and pervious areas of the same subcatchment, while GR can receive only the direct rainfall.

2.4 The model chain

2.4.1 The hydrologic model

The rainfall-runoff modelling was conducted using the dynamic hydrologic-hydraulic model SWMM. For runoff simulation, the study area was divided into subcatchments, each with its own pervious and impervious fraction (Rossman et al., 2010). Evapotranspiration was not included, as it is negligible when considering single events.

Based on the landuse dataset, the study area was divided into 230 subcatchments, with two subcatchment types: roads, covering 25 % of the study area, and residential, covering the remaining 75 %. The residential subcatchments summarise building blocks, including backyards and parks, instead of considering each building separately. The roads are defined as impervious, residential subcatchments as pervious, except the area covered by buildings. The subcatchments' average slope was calculated from the DEM. For infiltration, the SCS-Curve Number (CN) method (Mishra and Singh, 2003) was used. CNs for each subcatchment were assigned by combining the landuse dataset with the soil map, resulting in CNs ranging from 61–98, with an area-weighted mean CN of 91. A higher CN indicates higher impermeability and less infiltration.

Different from the remaining study area, the GI modules use the Green-Ampt method. For each subcatchment, the runoff generated by the impervious area is routed to the pervious area, and what remains is routed to the GI, if existing. As the sewer system is not publicly available, the gully water absorption was represented by increasing the depression storage of the roads.

https://doi.org/10.5194/egusphere-2025-5466
Preprint. Discussion started: 21 November 2025

Table 3. Bioretention system (BR), green roof (GR) and pervious pavement (PP) layer characteristics and usage.

	Parameter	BR	GR	PP	Unit
Surface layer	Berm height	150	50	50	mm
	Vegetation volume fraction	0	0	0	
	Surface roughness	0.2	0.2	0.013	Mannings n
	Surface slope	1	1	0.3	%
Pavement layer	Thickness			100	mm
	Void ratio			0.25	voids/solids
	Impervious surface fraction			0	
	Permeability			150	mm/h
	Clogging factor			0	
	Regeneration interval (days)			0	
	Regeneration fraction			0	
Soil layer	Thickness	500	150	200	mm
	Porosity	0.45	0.45	0.45	volume fraction
	Field capacity	0.1	0.1	0.1	volume fraction
	Wilting point	0.05	0.05	0.05	volume fraction
	Conductivity[a]	43	43	43	mm/h
	Conductivity slope	43	43	43	
	Suction head	60	60	60	mm
Storage layer	Thickness	400		500	mm
	Void ratio	0.65		0.65	voids/solids
	Seepage rate[b]	43		43	mm/h
	Clogging factor	0		0	
Drainage mat	Thickness		50		mm
	Void fraction		0.6		
	Roughness		0.3		Mannings n
GI usage	Area of each unit	2.5	7	25	m^2
	Surface width per unit	0	2.5	5	m
	Initially saturated	0	0	0	%
	Impervious area treated	100	0	100	%
	Pervious area treated	100	0	100	%

[a]Conductivity: saturated hydraulic conductivity.

[b]Seepage rate: rate at which water seeps into the native soil below the layer.

From the simulation results, the runoff hydrographs for each subcatchment were forwarded as input to the hydrodynamic model for subsequent modelling of the surface flood dynamics.

https://doi.org/10.5194/egusphere-2025-5466
Preprint. Discussion started: 21 November 2025

2.4.2 The hydrodynamic model

For the hydrodynamic simulations, the open source TELEMAC system is used. TELEMAC incorporates a 2D module that applies a finite element scheme with a semi-implicit solver on a triangulated mesh to solve the Shallow Water Equations (EDF, 2022).

The hydrodynamic model has an unstructured mesh with a resolution of 2 m which results in a total of approximately 768,000 nodes and 1,458,000 elements. Buildings cover around one third of the study area and are represented as holes in the model. The roughness coefficients are derived from the landuse data using the guidelines from the LUBW (LUBW, 2020). The topography is interpolated from the DEM.

The output hydrographs from the hydrologic model are represented in the hydrodynamic model by point sources and serve as the only input into the hydrodynamic model. The rivers Spree and Landwehrkanal are used as outlet boundary conditions in the northeast and south and east, respectively. The northwest boundary in the hydrodynamic model is moved outward compared to the hydrologic model to generate a less undulating model boundary line, which facilitates defining the boundary conditions here. The northwest boundary is defined as a closed wall, which prohibits water from leaving through this boundary, but does not create extensive backwater effects into the study area, as the model is spatially extended at this boundary. A more detailed description of the hydrodynamic model and the validation of the boundary conditions is provided in De Vos et al. (2024).

The maximum water depths and velocities are extracted from the simulation results and rastered with a 1×1 m resolution. These rasters are then forwarded to the building damage model.

2.4.3 The building damage model

In order to further assess the potential benefits of the GI measures, a building damage model was used. Despite the existence of numerous models to estimate flood damage to buildings, most were developed for typical riverine floods, whilst research has shown that different flood pathways show different damage patterns (Mohor et al., 2021; Gerl et al., 2016). Therefore, the „Flood Damage Estimation Tool“ (FlooDEsT; Samprogna Mohor et al., 2025) was adopted as it was specifically developed for urban pluvial floods.

The model was trained on survey data from past urban pluvial events between 2010 and 2016 in Germany (see Thieken et al., 2017). Using a recursive partitioning algorithm, the XGBoost (Chen and Guestrin, 2016), the model generates an additive ensemble of decision trees, where sequential trees are trained to correct the residual errors made by previous ones. The recursive partitioning algorithm is powerful at capturing non-linear relationships between the predictors (hazard characteristics, building characteristics) and the outcome variable (relative building damage). The input variables are a mix of physical and conceptual variables: water depth [m], flood intensity (in form of classes of people stability in flood waters), the presence of contaminants in the water, building area, building age, presence of a basement, and implemented adaptation measures in form of a score. For a detailed description of the input variables, especially how scores are calculated, consult Thieken et al. (2005). The model calibration performed well with a RMSE of relative building damage of 0.03 with the training data and 0.06 with the test data after 7 boosting rounds (i.e. additive trees).

https://doi.org/10.5194/egusphere-2025-5466
Preprint. Discussion started: 21 November 2025

In the application the model needs the maximum water depth and velocity from the hydraulic model (from which flood intensity is derived) and building information from cadastral data (either authoritative or OpenStreetMap data). Additionally, the tool uses smart random sampling to impute missing variables, such as building-level features, from the existing survey data distribution, which secures representativeness of buildings affected by this flood pathway, reducing exposure bias. Regardless of property size or market value, relative qualitative damage classes are provided, facilitating comparison.

2.5 Evaluating the flood mitigation impact of the retention scenarios

Combining all rain and retention scenarios described in section 2.3, a total of 70 scenarios were defined. After processing them through the model chain, the flood mitigation impact of the GI scenarios was assessed using the following variables: runoff total from the hydrologic model, percentage of the study area with maximum water depth > 10 cm from the hydrodynamic model and the percentage of damaged buildings (see Figure 1).

In order to assess the flood mitigation impact comprehensively, from each of these variables, the following three indices were calculated: First, the absolute reduction compared to the base scenario (eq. 1), second, the relative reduction (as percentage, eq. 2) and third, the absolute reduction per square meter of GI (eq. 3), with X for the respective variable, such as runoff total or percentage of damaged buildings. X_{base} represents the base scenario, X_{scen} the considered retention scenario. For the gully scenarios, only eq. 1 and 2 can be applied, as no spatial extent was assigned to the gullies.

$$Red_{abs} = X_{base} - X_{scen} \tag{1}$$

$$Red_{rel} = \frac{X_{base} - X_{scen}}{X_{base}} \cdot 100 \tag{2}$$

$$Red_{abs,GI} = \frac{X_{base} - X_{scen}}{GI_{share}} \tag{3}$$

In the literature, relative reduction is the most common index. However, it gives a large emphasis on the flood reduction of small rainfall events. Absolute reduction was added to see the actual retention of the scenarios, using the same unit as the considered variable. However, the possible range for absolute flood reduction is limited by small values of the considered variables for the smaller rain events. Additionally, the GI implementation degree influences a lot the result. Therefore, absolute retention per square meter of GI was included as well.

Flow velocity in combination with water depth is crucial for damage modelling. However, due to the flat topography of the study area, flow velocities are rather low. Hence, flow velocity was not used as variable for the flood mitigation impact assessment.

https://doi.org/10.5194/egusphere-2025-5466
Preprint. Discussion started: 21 November 2025

3 Results

This section begins with the results of the hydrologic, hydrodynamic and building damage models. Then, flood mitigation is evaluated according to the absolute reduction, relative reduction and, finally, regarding the spatial efficiency of the studied GI types.

3.1 Pluvial flood response through the model chain

Figure 3 gives an overview of the results of the model chain, showing event runoff in mm (first row), the percentage of the study area with a maximum water depth > 10 cm (second row) and the percentage of damaged buildings for the different rainfall and retention scenarios (see also Table A1).

Referring to the rainfall scenarios, the first three columns of Figure 3 show the KOSTRA events, with the medium retention scenarios in the first, the maximum retention scenarios in the second and the combined retention scenarios in the third column. For a better visibility of the KOSTRA events, the extreme event with a rain total of 100 mm was plotted with a different y-axis separately in the fourth column. The base and gully scenarios are shown in all columns to improve comparability.

In general, all retention scenarios show less runoff, flooded area and building damage than the base scenario. The maximum GI scenarios outperform the medium GI scenarios and the combined scenarios outperform all single GI scenarios. Among the single GI scenarios, BR produces the lowest runoff. Regarding the flooded area and damaged buildings, BR is also the strongest among the single GI scenarios with maximum extent, however, at the medium scenarios, PP outperforms BR in most events. The gully scenario shows the lowest flood mitigation impact, only for the 1-year event, it outperforms GR and PP, and among the medium scenarios, it outperforms GR at the flooded area and damaged buildings for several of the smaller events.

The combined scenario of GR_{max} and BR_{max} provides the highest flood mitigation. Regarding the 49 mm event, it reduces the runoff and area with flood depth > 10 cm to values below the 25 mm base scenario. The damaged buildings drop even below the 15 mm base scenario.

In the following sections, we will look at the flood mitigation impact indices defined in section 2.5 for a more comprehensive performance evaluation.

3.2 Absolute flood reduction

Absolute flood reduction (Figure 4a–c) is in most rain scenarios the highest for the combined GI scenarios. However, in some events, they are partially outperformed by other retention scenarios. For example, BR_{max} is among the scenarios with the highest reductions for the smaller events, for the larger events, its impact reduces. With increasing event rainfall, we observe a decrease in the reduction of damaged buildings. The low damage class constitutes in all scenarios the largest share of the total number of damaged buildings.

https://doi.org/10.5194/egusphere-2025-5466
Preprint. Discussion started: 21 November 2025

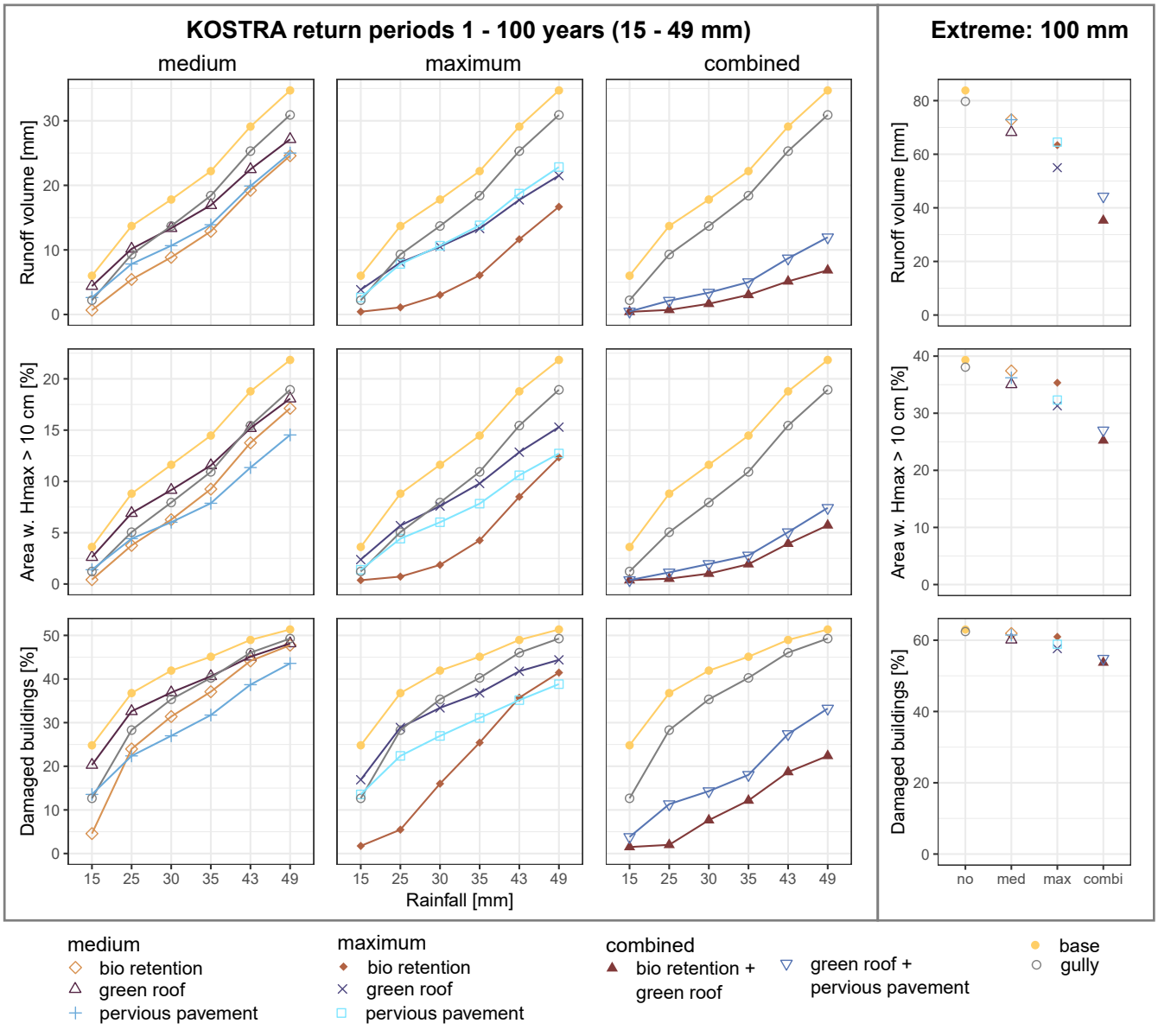

Figure 3. Results of the model chain: runoff total, area with maximum water depth (Hmax) over 10 cm and percentage of damaged buildings for six rain events (KOSTRA return periods 1, 5, 10, 20, 50, 100 years and an extreme event with 100 mm), comparing base and gully scenario to the medium, maximum and combined GI scenarios.

https://doi.org/10.5194/egusphere-2025-5466
Preprint. Discussion started: 21 November 2025

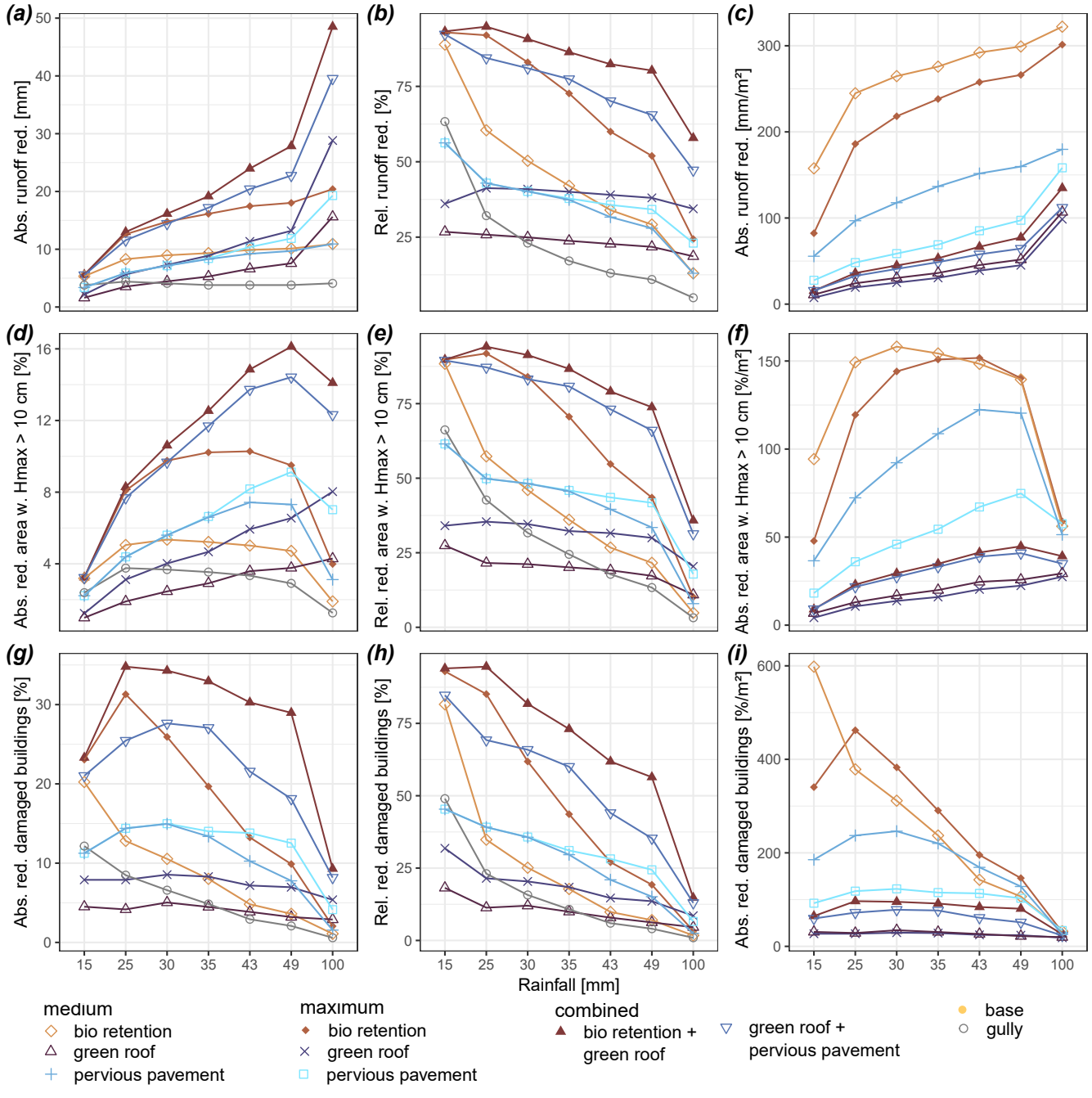

Figure 4. Absolute (a,d,g) and relative (b,e,h) flood mitigation and spatial efficiency (c,f,i) of the assessed rainfall and retention scenarios: runoff total (a,b,c), area with maximum water depth (Hmax) > 10 cm (d,e,f) and percentage of damaged buildings (g,h,i).

https://doi.org/10.5194/egusphere-2025-5466
Preprint. Discussion started: 21 November 2025

3.3 Relative flood reduction

Relative flood reduction (Figure 4d–f) results in a reduction of runoff total by 4.9–94.8 %. The flooded area with maximum water depth > 10 cm reduces by 3.2–94.1 %. Building damage is reduced by 0.9–94.6 %, with 0.8–94.6 % in the low, 0.0–96.0 % in the medium, -8.3–100 % in the high and 0.0–100.0 % in the very high damage class.

For most retention scenarios and variables, relative flood reduction decreases clearly with increasing rainfall, only for the GR scenarios (GR_{med} and GR_{max}) this trend is less apparent. For most events and variables, the combined scenarios and BR_{max} show the strongest results. The gully scenarios show a medium performance for the 1-year event and then decrease with increasing event rainfall to quite small absolute and relative flood reduction values compared to the GI retention scenarios.

3.4 Spatial efficiency of the different green infrastructure types

Absolute flood reduction per square meter of GI (Figure 4g–i) allows to compare the spatial efficiency of the different GI scenarios. Regarding runoff, the reduction per square meter increases with increasing rainfall and BR_{med} shows at each event the highest reduction, followed by BR_{max} and PP_{med}. Area with maximum water depth > 10 cm first increases and after a peak at the events with 30–43 mm decreases with increasing event total. Again, BR_{med}, BR_{max} and PP_{med} achieve the highest reduction per square meter. Only at the 100 mm event PP_{max} outperforms BR_{med}, BR_{max} and PP_{med}. The building damage reduction is the smallest for the 100 mm event.

4 Discussion

4.1 Green infrastructure scenarios - realistic or too ambitious?

The results of our study show that, with an intense implementation of GI, high absolute and relative flood mitigation can be achieved. However, retrofitting GI in a historically grown city is much more challenging then designing a fully new housing development.

To address the question of how realistic the implementation of the different investigated GI scenarios is in practice, we compare our scenarios to those elaborated by Knoche et al. (2024). They conducted workshops with the Senate Department for Urban Mobility, Transport, Climate Protection and the Environment (SenMVKU), the Berlin water supply and drainage company (Berliner Wasserbetriebe; BWB), the Berlin rainwater agency (Berliner Regenwasseragentur) and two Berlin district authorities in order to define realistic stormwater management strategies. These scenarios included different types of GI, such as green roofs and unsealing of parking places, to achieve a reduction of sewage overflows in the area of Berlin drained by a combined sewer system.

Within a timeframe of 10 years, Knoche et al. (2024) suggest an unsealing of 5.5 % of the study area, with 1.5 % located on streets and 4 % on properties. Accordingly, both BR scenarios are realistic to be implemented within the next 10 years.

https://doi.org/10.5194/egusphere-2025-5466
Preprint. Discussion started: 21 November 2025

Within 30 years, an unsealing of 27.5 % is suggested, with 4.5 % on streets and 22.5 % on properties. If we do not strictly stick to the distribution among streets and properties but on the total unsealed area, this means that GR_{med}, PP_{med} and PP_{max} are realistic within the next 30 years.

The 3 scenarios with the largest conversion to GI (GR_{max}, GR_{max}+PP_{med} and BR_{max}+GR_{max}) require reductions of impervious area beyond those elaborated by Knoche et al. (2024) for a timeframe of 30 years. Hence, their realisation within the next decades seems unrealistic.

4.2 Space efficiency versus continuation of former land use

As shown in this study, BR is the GI measure that provides the highest flood mitigation per square meter. Nevertheless, when we discuss space efficiency, we also need to take into account whether the GI implementation impedes other uses of the space. In the case of GR, the usability of the building does not change. For PP, at least parking lots and residential roads with reduced speed and traffic load continue providing the same functionality. In contrast, BR requires the surface area to be free from buildings and traffic. Still, GI can provide further ecosystem services beyond flood mitigation by increasing groundwater recharge (Bhaskar et al., 2018) and, if a vegetation cover is present, contribute to the mitigation of urban heat stress (Cristiano et al., 2022; Watrin et al., 2019) through evapotranspirative cooling, increase biodiversity (Monberg et al., 2018) and improve the aesthetic value of the urban environment.

4.3 Comparison of the simulated flood mitigation to previous studies

Due to the nature of a scenario analysis, there are no measurement data for validating the flood mitigation impact of the GI scenarios modelled in this study. Instead, we can compare our results to data from the literature. As surface runoff is the most directly affected by the GI measures, we will focus on this variable in the following section. Nevertheless, surface flooding and building damage will also be considered.

4.3.1 Runoff retention

In order to compare the GI impact on runoff volume with other studies, we selected examples from those studies reviewed in Dobkowitz et al. (2025) based on similarity of study area, event and retention scenario characteristics. More specifically, we considered only events with a duration of 0.5–2 h and rain totals of 10–60 mm and 90–110 mm, as the rain totals modelled in our study range from 15–49 mm and 100 mm was added as an extreme event. Regarding the area covered by GI, we selected those studies with 1–10 % of the study area for BR, with 10–45 % for GR and with 4–20 % for PP. Finally, the impervious area for selecting a study was restricted to 20–50 % for GR and 15–70 % for PP. Due to the smaller amount of available studies, this last criterion was not applied when selecting BR studies. The selection resulted in 25 events from 6 studies, relative runoff reduction from these studies is shown in Table 4:

- Ercolani et al. (2018) used the model smart-green (MOBIDIC-U and a QGIS plugin) to investigate GR in a 1.9 km^2 study area in Milan, Italy (MAP 800 mm).

https://doi.org/10.5194/egusphere-2025-5466
Preprint. Discussion started: 21 November 2025

- Fu et al. (2020) coupled SWMM and Hydrus-1D to model PP in a 3.3 km^2 study area in Xiamen, China (MAP 1413 mm).
- Hua et al. (2020) also studied PP, using the model MIKE URBAN for a 7.4 km^2 study area in Chaohu, China (MAP 1307 mm).
- Peng et al. (2019) investigated GR with SWMM in a 0.044 km^2 study area in Fuzhou, China (MAP 1500 mm).
- Schlea et al. (2014) investigated BR with an experimental study, using a rain gauge, graduaded containers for runoff and drainage measurements and piezometers for water table changes. This setup was used in a 869 m^2 study area located in Westerville, USA (MAP 1105 mm)
- Zhang et al. (2020) modeled BR with SWMM in a 6.07 km^2 study are in Kyoto, Japan (MAP 1677 mm).

Table 4. Comparison of relative runoff reduction with other studies.

GI Scenario	Rainfall scenario	Runoff reduction [%] in this study	Runoff reduction [%] in reviewed studies	Reference
Bioretention system				
BR_{med}	1 year	89	33	Schlea et al. 2014
BR_{max}	100 years	52	14	Zhang et al. 2020
BR_{max}	100 mm	24	14	Zhang et al. 2020
Green roof				
GR_{med}	1 year	27	44–59	Ercolani et al. 2018
GR_{med}	10 years	25	17–52	Ercolani et al. 2019
GR_{med}	20 years	24	35–49	Ercolani et al. 2020
$GR_{med\ or\ max}$	20 years	24–40	31	Peng et al. 2019
GR_{med}	50 years	23	13–24	Ercolani et al. 2022
$GR_{med\ or\ max}$	100 years	22–38	30	Peng et al. 2019
$GR_{med\ or\ max}$	100 mm	19–34	26–27	Peng et al. 2019
Pervious pavement				
PP_{med}	20 years	37	10	Hua et al. 2020
PP_{med}	50 years	32	9	Hua et al. 2021
PP_{max}	50 years	36	9	Fu et al. 2020
PP_{med}	100 years	28	10	Hua et al. 2020
PP_{med}	100 mm	13	1	Fu et al. 2020
PP_{max}	100 mm	23	2	Fu et al. 2021

https://doi.org/10.5194/egusphere-2025-5466
Preprint. Discussion started: 21 November 2025

Regarding BR, runoff reduction in the reviewed studies is 44–73 % lower than in our study. A possible explanation for this difference is that the impervious area is 46–75 % higher in these studies. This increases runoff formation in the remaining study area and reduces the relative runoff reduction of BR. The BR extent of the event from Schlea et al. (2014) is 38 % lower than in our study, which also decreases the runoff retention. However, for the two other compared events, the BR extent shows no significant difference. Rain totals are with at most 15 % not significantly higher in the compared studies.

For GR, most of the examples from Ercolani et al. (2018) result in much higher runoff reduction. This can be a result of the 36–49 % lower imperviousness of the study area. In terms of the GR extent, Ercolani et al. (2018) has two settings, with GR covering 10.3 or 15.4 % of the study area. In the first case, this is 29 % less GR then in the GR_{med} scenario and results in 43 % less to 64 % more runoff reduction. In the second case, this is 5 % more GR then in the GR_{med} scenario, resulting in 6–120 % more runoff reduction.

With respect to the GR extent, the scenarios from Peng et al. (2019) are between GR_{med} and GR_{max}, i.e. the GR extent is 48 % larger than GR_{med} and 26 % smaller than GR_{max}. The imperviousness of the study area is closer to GR_{med}, as it is 22 % higher than GR_{med} and 91 % higher than GR_{max}. The runoff reduction from Peng et al. (2019) turns out to be centred between the runoff reduction of the corresponding scenarios, with 30–45 % more runoff reduction than GR_{med} and 21–24 % less runoff reduction than GR_{max}.

PP shows less runoff reduction in both reviewed studied. When comparing to Hua et al. (2020), the 63–72 % lower runoff reduction can be caused by the 42 % higher imperviousness of the study area compared to PP_{med} and 28 % smaller PP extent. However, with regard to Fu et al. (2020), the impervious area is 7–25 % smaller and the PP extent 9–63 % larger than in the corresponding scenarios of this study. Still, runoff retention is 75–92 % lower. This is even more surprising, as the saturated hydraulic conductivity of the different layers of the upper 35 cm is with 133–606 mm/h much higher than in this study (43–150 mm/h, see Table 3). Only the plain fill below has with 10.2 mm/h a lower conductivity.

4.3.2 Flood volume reduction

Neumann et al. (2024) and Tügel et al. (2025) investigated flood volume reduction by GI in Berlin. Neumann et al. (2024) studied the impact of extensive GR, intensive GR and GR with enhanced retention (retention roof), among other GI measures. They investigated the same study area as our study, using the software InfoWorksICM (Autodesk, 2023). Tügel et al. (2025) coupled the models hms^{++} (Steffen and Hinkelmann, 2023) with SWMM and assessed the impact of retention roofs and gullies in a 13 km^2 study area in the centre of Berlin, with 35 % roof and 16 % road surfaces.

Despite the similarity of the study areas, GI extents and rain event characteristics, comparability is limited by the use of different measures of flood volume. While Neumann et al. (2024) defined flood volume as the sum of maximum water level in each mesh element with at least 10 cm water depth, Tügel et al. (2025) used the sum of maximum water level of all mesh elements. In our study, the percentage of the study area with a maximum water level of at least 10 cm is used. Besides, the reviewed GR scenarios and the reference base scenarios are combined with the sewer system in most cases, whereas our study uses GI and base scenarios without gullies.

https://doi.org/10.5194/egusphere-2025-5466
Preprint. Discussion started: 21 November 2025

Comparing relative flood reduction despite these limitations in comparability, we see that Neumann et al. (2024) reports the most similar results for the 100-year event, with a flood volume reduction of 32 % for extensive GR and 34 % for intensive GR and retention roofs. This is very close to GR_{max} with a 30 % reduced area with maximum water level > 10 cm.

For the 100 mm event, flood flood volume reduction according to Neumann et al. (2024) is 14 % for extensive GR and 34 % for intensive GR and retention roofs, while GR_{max} results in a reduction of the area with maximum water level > 10 cm of 20 %. It is noticeable that in the study of Neumann et al. (2024) there is hardly any difference in relative flood volume reduction between intensive GR and retention roof including the 100-year and the 100 mm event, showing that the 100-year event does not make full use of the retention potential of those GR types.

Regarding the gully water retention compared to a base scenario without drainage system, Tügel et al. (2025) reports a much larger impact of the drainage system than our study. For the 100-year event, Tügel et al. (2025) results in 31 % reduction of flood volume while our gully scenario results in 13 % less area with maximum water level >10 cm. For the 100 mm rain event the relative difference still increases, with 26 % (Tügel et al., 2025) compared to 3 % from our gully scenario. Possible explanations for the difference are the different study areas, different models and model parametrisations or the different implementation of the drainage system itself. While Tügel et al. (2025) used the drainage system model from BWB, which is a restricted dataset, in our study a simplified approach was used by defining gully water absorption due to the official drainage system requirements. Alternatively, a virtual drainage system based on open data could be created using the method presented by Montalvo et al. (2024). It depends on the use case, if the additional effort for the drainage model setup and increase in run time is worth for including a more complex drainage system in the model chain.

4.3.3 Building damage mitigation

Staccione et al. (2024) tested the effect of GI (GR and green open spaces) on building damage reduction in Milan (Italy), considering progressive higher intensities of green conversion and different rainfall scenarios. Overall, it was found that GI can reduce flood impact, but proportionally, the higher gains occur for lower rain intensities. The 100-year event corresponds to 54.7 mm in 1 hour. A 100 % implementation of GR potentially reduces building damage by ca. 21 % for the 100-year event (or ca. 39 % of the expected annual damage (EAD), integrating all rainfall scenarios), whilst a conversion of 50 % to GR reduces damage by ca. 17 % for the 100-year event (32 % reduction of EAD). In turn, a conversion of 25 % of potential green areas reduces building damage by ca. 13 % for the 100-year event (or 25 % reduction of EAD).

Our analyses do not convey absolute monetary values, but relative ones. Yet, our 100-year scenario with 100 % GR (GR_{max}) would reduce the number of damaged buildings in any damage class by 14 % and the number of buildings suffering medium damage or higher by 67 %. GR_{med} in turn could reduce the number of damaged buildings by respectively 6 % (any damage level) or 42 % (medium or higher damage).

Locatelli et al. (2020) show that a combination of GI in Barcelona (Spain), reducing the impervious area by 14 % could almost halve the EAD (46 % reduction); whilst an impervious area reduction of 2 % in Badalona (a town next to Barcelona) would reduce EAD by less than 4 %.

https://doi.org/10.5194/egusphere-2025-5466
Preprint. Discussion started: 21 November 2025

Although we have not tested an equivalent combination of GI, scenarios GR_{med} and PP_{max} have similar percentages of GI area to the Barecelona case study, with 14.6 % and 12.2 %, respectively. The PP_{max} scenario for the 100-year event would reduce the number of damaged buildings by 24 % or reduce buildings with medium or higher damage by 12 %. The BR_{med} scenario has with a GI area of 3.4 % a similar extent to the Badalona case study and results in a reduction of damaged buildings by 7 % or a reduction of buildings with medium and higher damage by 26 %.

5 Conclusions

This study investigates the potential of GI in urban pluvial flood mitigation by setting up a multi-scenario analysis framework that integrates hydrological, hydrodynamic and building damage models. With a case study located in the centre of Berlin, the impact of different retention and rainfall scenarios on runoff, maximum water depth and building damage was assessed. Absolute and relative flood mitigation and spatial efficiency of GI served as indices to evaluate the scenarios.

From this study, we can conclude that the more impervious area is converted to GI, the more flood mitigation can be achieved. All of the modelled GI scenarios reduce flooding compared to the base scenario and also outperform the gully scenario, at least for the larger rain events.

The combined scenario GR_{max}+BR_{max} requires with 36 % the highest percentage of the study area and achieves the highest absolute and relative flood mitigation at all three modelling steps.

Both BR scenarios can compete with the combined GI scenarios for the smallest events, however, the relative reduction decreases strongly with increasing rain totals. Regarding space efficiency, the BR scenarios show the best performance but it requires a change of land use, different from GR and PP.

Relative flood mitigation decreases with increasing rain totals for all GI scenarios and at all modelling steps. In contrast, absolute flood mitigation behaves differently: While the absolute runoff reduction is highest at the 100 mm event, the area with maximum water depth > 10 cm decreases the most at the 49 mm event (return period 100 years) and building damage at 25–30 mm (return period 5–10 years).

The comparison of the space needed for GI to Knoche et al. (2024) showed that several of the scenarios investigated in this study are realistic to be implemented within a timeframe of 10 years (BR_{med}, BR_{max}) or 30 years (GR_{med}, PP_{med}, PP_{max}. However, the GI scenarios with the largest extents (GR_{max}, GR_{max}+PP_{med} and BR_{max}+GR_{max}) are probably not feasible within the next 30 years.

Comparing the flood mitigation potential of GI to the reviewed studies shows that the results range from similar to very different results. For example, runoff reduction from GR differed much less between our study and the reviewed studies than from PP. In some cases, the study area and GI characteristics help to understand the differences. In other cases it is not clear, as many different parameters, such as the applied models themselves and the input data used for model setup impact the modelling results.

While more GI increases flood mitigation, limited urban space and financial costs for construction and maintenance impede the implementation of larger extents of GI, especially in old city centres. In new city developments, the implementation of GI

https://doi.org/10.5194/egusphere-2025-5466
Preprint. Discussion started: 21 November 2025

can reduce the needed conventional drainage infrastructure and thereby require no additional costs. The evaluation of financial feasibility depends on which aspects are taken into account. This might include the various further benefits of GI, such as urban heat mitigation and increased biodiversity but also the costs of damage to buildings and other infrastructure that can be avoided.

435 For a more comprehensive evaluation of different GI scenarios, in future studies it would be beneficial to include the costs of GI and also simulate longer time series in order to evaluate the impact of GI for several years, including projected climate change scenarios.

Appendix A: Results of the model chain

Table A1: Results of the model chain for all investigated design rainfall and retention scenarios.

Return period	Scenario	Rain total [mm]	Runoff volume [mm]	Area w. Hmax > 10 cm [%]	Buildings low damage [%]	Buildings medium damage [%]	Buildings high damage [%]	Buildings very high damage [%]	Damaged buildings [%]
1y	Base	14.8	6.0	3.6	24.5	0.28	0.03	0.03	24.8
5y	Base	25.0	13.7	8.8	36.1	0.59	0.06	0.06	36.8
10y	Base	29.9	17.8	11.6	40.9	0.87	0.06	0.06	41.9
20y	Base	35.0	22.2	14.5	43.9	1.09	0.09	0.06	45.1
50y	Base	42.7	29.1	18.8	47.2	1.55	0.09	0.06	49.0
100y	Base	48.9	34.7	21.8	49.2	1.93	0.09	0.12	51.4
100mm	Base	100.0	83.8	39.3	56.3	5.84	0.37	0.50	63.0
1y	Gully	14.8	2.2	1.2	12.4	0.25	0.00	0.03	12.7
5y	Gully	25.0	9.3	5.0	27.7	0.53	0.03	0.06	28.3
10y	Gully	29.9	13.7	7.9	34.4	0.84	0.03	0.06	35.3
20y	Gully	35.0	18.4	10.9	39.0	1.09	0.09	0.06	40.3
50y	Gully	42.7	25.3	15.4	44.4	1.46	0.09	0.06	46.0
100y	Gully	48.9	30.9	18.9	47.3	1.77	0.09	0.12	49.3
100mm	Gully	100.0	79.7	38.1	55.8	5.81	0.37	0.47	62.4
1y	BRmed	14.8	0.7	0.4	4.4	0.12	0.00	0.00	4.6
5y	BRmed	25.0	5.4	3.8	23.6	0.28	0.06	0.03	24.0
10y	BRmed	29.9	8.8	6.3	30.8	0.50	0.06	0.03	31.4
20y	BRmed	35.0	12.9	9.2	36.2	0.78	0.06	0.03	37.1

https://doi.org/10.5194/egusphere-2025-5466
Preprint. Discussion started: 21 November 2025

Table A1: Results of the model chain for all investigated design rainfall and retention scenarios.

Return period	Scenario	Rain total [mm]	Runoff volume [mm]	Area w. Hmax > 10 cm [%]	Buildings low damage [%]	Buildings medium damage [%]	Buildings high damage [%]	Buildings very high damage [%]	Damaged buildings [%]
50y	BRmed	42.7	19.2	13.8	42.9	1.12	0.09	0.06	44.1
100y	BRmed	48.9	24.6	17.1	46.2	1.43	0.09	0.06	47.7
100mm	BRmed	100.0	72.9	37.4	55.8	5.28	0.40	0.40	61.9
1y	BRmax	14.8	0.4	0.4	1.7	0.03	0.00	0.00	1.7
5y	BRmax	25.0	1.1	0.7	5.3	0.09	0.00	0.03	5.5
10y	BRmax	29.9	3.0	1.9	15.8	0.16	0.06	0.03	16.0
20y	BRmax	35.0	6.1	4.2	24.9	0.44	0.06	0.03	25.4
50y	BRmax	42.7	11.6	8.5	34.9	0.75	0.06	0.03	35.7
100y	BRmax	48.9	16.7	12.3	40.3	1.06	0.09	0.06	41.5
100mm	BRmax	100.0	63.4	35.3	55.3	5.00	0.31	0.34	61.0
1y	GRmed	14.8	4.4	2.6	20.2	0.06	0.03	0.00	20.3
5y	GRmed	25.0	10.2	6.9	32.2	0.40	0.03	0.00	32.6
10y	GRmed	29.9	13.4	9.2	36.4	0.47	0.03	0.03	36.9
20y	GRmed	35.0	16.9	11.6	39.9	0.65	0.03	0.06	40.6
50y	GRmed	42.7	22.5	15.2	44.1	0.90	0.06	0.06	45.1
100y	GRmed	48.9	27.1	18.1	46.9	1.12	0.06	0.06	48.2
100mm	GRmed	100.0	68.2	35.0	55.8	3.92	0.19	0.22	60.1
1y	GRmax	14.8	3.8	2.4	16.8	0.03	0.03	0.00	16.9
5y	GRmax	25.0	8.0	5.7	28.6	0.25	0.03	0.00	28.9
10y	GRmax	29.9	10.5	7.6	33.1	0.28	0.03	0.00	33.4
20y	GRmax	35.0	13.3	9.8	36.5	0.28	0.03	0.00	36.8
50y	GRmax	42.7	17.7	12.8	41.2	0.53	0.03	0.00	41.8
100y	GRmax	48.9	21.5	15.3	43.7	0.65	0.03	0.03	44.4
100mm	GRmax	100.0	55.0	31.3	54.5	2.89	0.09	0.12	57.6
1y	PPmed	14.8	2.6	1.4	13.2	0.28	0.00	0.03	13.6
5y	PPmed	25.0	7.8	4.4	21.8	0.53	0.03	0.06	22.4
10y	PPmed	29.9	10.7	6.0	26.1	0.78	0.06	0.06	27.0

https://doi.org/10.5194/egusphere-2025-5466
Preprint. Discussion started: 21 November 2025

Table A1: Results of the model chain for all investigated design rainfall and retention scenarios.

Return period	Scenario	Rain total [mm]	Runoff volume [mm]	Area w. Hmax > 10 cm [%]	Buildings low damage [%]	Buildings medium damage [%]	Buildings high damage [%]	Buildings very high damage [%]	Damaged buildings [%]
20y	PPmed	35.0	13.9	7.9	30.5	1.06	0.09	0.06	31.7
50y	PPmed	42.7	19.9	11.3	37.1	1.43	0.09	0.06	38.7
100y	PPmed	48.9	25.0	14.5	41.7	1.71	0.09	0.12	43.6
100mm	PPmed	100.0	72.9	36.2	55.1	5.50	0.37	0.47	61.5
1y	PPmax	14.8	2.6	1.4	13.2	0.28	0.00	0.03	13.6
5y	PPmax	25.0	7.8	4.4	21.8	0.53	0.03	0.06	22.4
10y	PPmax	29.9	10.7	6.0	26.0	0.78	0.06	0.06	27.0
20y	PPmax	35.0	13.8	7.8	29.9	1.06	0.09	0.06	31.1
50y	PPmax	42.7	18.7	10.6	33.6	1.43	0.09	0.06	35.2
100y	PPmax	48.9	22.8	12.7	36.9	1.68	0.09	0.12	38.8
100mm	PPmax	100.0	64.5	32.3	52.8	5.32	0.34	0.47	58.9
1y	BRmax+GRmax	14.8	0.4	0.4	1.5	0.03	0.00	0.00	1.5
5y	BRmax+GRmax	25.0	0.7	0.5	2.0	0.03	0.00	0.00	2.0
10y	BRmax+GRmax	29.9	1.7	1.0	7.6	0.06	0.03	0.00	7.6
20y	BRmax+GRmax	35.0	3.0	1.9	12.1	0.06	0.03	0.00	12.2
50y	BRmax+GRmax	42.7	5.1	3.9	18.6	0.06	0.03	0.00	18.7
100y	BRmax+GRmax	48.9	6.8	5.7	22.2	0.12	0.03	0.00	22.4
100mm	BRmax+GRmax	100.0	35.3	25.2	51.6	1.99	0.03	0.09	53.7
1y	GRmax+PPmed	14.8	0.5	0.4	3.8	0.03	0.00	0.00	3.8
5y	GRmax+PPmed	25.0	2.1	1.1	11.2	0.16	0.00	0.00	11.3
10y	GRmax+PPmed	29.9	3.4	1.9	14.1	0.12	0.03	0.00	14.3
20y	GRmax+PPmed	35.0	5.0	2.8	17.8	0.19	0.03	0.00	18.0
50y	GRmax+PPmed	42.7	8.7	5.0	26.9	0.44	0.03	0.00	27.4
100y	GRmax+PPmed	48.9	12.0	7.4	32.6	0.59	0.03	0.03	33.2
100mm	GRmax+PPmed	100.0	44.3	27.0	52.0	2.61	0.09	0.12	54.8

https://doi.org/10.5194/egusphere-2025-5466
Preprint. Discussion started: 21 November 2025

Author contributions. Conceptualization and supervision: AB. Methodology: LFDV, OS, GSM, SL, SD. Formal analysis: DCJ, SD. Visualization: SD. Writing: The original draft was prepared by SD, LFDV, GSM and SL, review and editing by SD, LFDV, GSM, SL, OS and AB.

Competing interests. The authors declare that they have no conflict of interest.

Acknowledgements. The Scientific colour map managua (Crameri, 2018) is used in this study to prevent exclusion of readers with colour-vision deficiencies (Crameri et al., 2020).

https://doi.org/10.5194/egusphere-2025-5466
Preprint. Discussion started: 21 November 2025

References

ALKIS: Amtliches Liegenschaftskatasterinformationssystem (ALKIS), https://fbinter.stadt-berlin.de/fb/index.jsp, accessed: 2024-10-01, 2024.

ATKIS: Digital Terrain Model, https://fbinter.stadt-berlin.de/fb/berlin/service_intern.jsp?id=a_dgm@senstadt&type=FEED, accessed: 2024-10-01, 2024.

Autodesk: InfoWorks ICM, https://www.autodesk.com/, 2023.

Berghäuser, L., Schoppa, L., Ulrich, J., Dillenardt, L., Jurado, O. E., Passow, C., Mohor, G. S., Seleem, O., Petrow, T., and Thieken, A.: Starkregen in Berlin, Tech. rep., Institut für Umweltwissenschaften und Geographie, 2021.

Bhaskar, A. S., Hogan, D. M., Nimmo, J. R., and Perkins, K. S.: Groundwater recharge amidst focused stormwater infiltration, Hydrological Processes, 32, 2058–2068, 2018.

BKG: WMS Hinweiskarte Starkregengefahren, https://gdz.bkg.bund.de/index.php/default/wms-hinweiskarte-starkregengefahren-wms-starkregen.html, 2025.

Bürger, G., Pfister, A., and Bronstert, A.: Temperature-driven rise in extreme sub-hourly rainfall, Journal of Climate, 32, 7597–7609, 2019.

Bürger, G., Pfister, A., and Bronstert, A.: Zunehmende Starkregenintensitäten als Folge der Klimaerwärmung: Datenanalyse und Zukunftsprojektion, Hydrologie und Wasserbewirtschaftung: HyWa= Hydrology and water resources management, Germany/Hrsg.: Fachverwaltungen des Bundes und der Länder, 65, 262–271, 2021.

Caretta, A. M. M. A., Arfanuzzaman, R. B. M., Morgan, S. M. R., Kumar, M., et al.: Water. In: Climate Change 2022: Impacts, Adaptation, and Vulnerability. Contribution of Working Group II to the Sixth Assessment Report of the Intergovernmental Panel on Climate Change, Cambridge University Press, Cambridge, UK and New York, NY, USA, 2022.

Chen, T. and Guestrin, C.: XGBoost: A Scalable Tree Boosting System, in: Proceedings of the 22nd ACM SIGKDD International Conference on Knowledge Discovery and Data Mining, pp. 785–794, ACM, San Francisco California USA, ISBN 978-1-4503-4232-2, https://doi.org/10.1145/2939672.2939785, 2016.

Crameri, F.: Scientific colour maps, Zenodo, 10, 5281, 2018.

Crameri, F., Shephard, G. E., and Heron, P. J.: The misuse of colour in science communication, Nature communications, 11, 5444, 2020.

Cristiano, E., Annis, A., Apollonio, C., Pumo, D., Urru, S., Viola, F., Deidda, R., Pelorosso, R., Petroselli, A., Tauro, F., et al.: Multilayer blue-green roofs as nature-based solutions for water and thermal insulation management, Hydrology Research, 53, 1129–1149, 2022.

De Vos, L. F., Rüther, N., Mahajan, K., Dallmeier, A., and Broich, K.: Establishing Improved Modeling Practices of Segment-Tailored Boundary Conditions for Pluvial Urban Floods, Water, 16, 2448, https://doi.org/10.3390/w16172448, 2024.

Dobkowitz, S., Bronstert, A., and Heistermann, M.: Water retention by green infrastructure to mitigate urban flooding: a meta-analysis, Urban Water Journal, pp. 1–16, 2025.

DWA: DWA-Regelwerk. Merkblatt DWA-M 165-1, 2021.

DWD: Heavy rain catalogue of the German National Meteorological Service, KOSTRA-DWD, version 2020, https://www.dwd.de/DE/leistungen/kostra_dwd_rasterwerte/kostra_dwd_rasterwerte.html, 2020a.

DWD: KOSTRA-DWD, version 2020, tables for download, https://www.openko.de/kostra-dwd-2020-tabellen-kostenlos-herunterladen/, 2020b.

DWD: Vieljährige Mittelwerte, https://www.dwd.de/DE/leistungen/klimadatendeutschland/vielj_mittelwerte.html, accessed: 2025-09-09, 2023.

https://doi.org/10.5194/egusphere-2025-5466
Preprint. Discussion started: 21 November 2025

EDF: TELEMAC-2D: User Manual. Version v8p4, 2022.

EPA, U.: Storm Water Management Model (SWMM), https://www.epa.gov/water-research/storm-water-management-model-swmm, 2023.

Ercolani, G., Chiaradia, E. A., Gandolfi, C., Castelli, F., and Masseroni, D.: Evaluating performances of green roofs for stormwater runoff mitigation in a high flood risk urban catchment, Journal of Hydrology, 566, 830–845, 2018.

Fletcher, T. D., Andrieu, H., and Hamel, P.: Understanding, management and modelling of urban hydrology and its consequences for receiving waters: A state of the art, Advances in water resources, 51, 261–279, 2013.

Fletcher, T. D., Shuster, W., Hunt, W. F., Ashley, R., Butler, D., Arthur, S., Trowsdale, S., Barraud, S., Semadeni-Davies, A., Bertrand-Krajewski, J.-L., et al.: SUDS, LID, BMPs, WSUD and more–The evolution and application of terminology surrounding urban drainage, Urban water journal, 12, 525–542, 2015.

Fu, X., Liu, J., Shao, W., Mei, C., Wang, D., and Yan, W.: Evaluation of permeable brick pavement on the reduction of stormwater runoff using a coupled hydrological model, Water, 12, 2821, 2020.

GDV: Naturgefahren. Starkregenbilanz 2002 bis 2021: Bundesweit 12,6 Milliarden Euro Schäden, https://www.gdv.de/gdv/medien/medieninformationen/starkregenbilanz-2002-bis-2021-bundesweit-12-6-milliarden-euro-schaeden-137444, 2023.

Gerl, T., Kreibich, H., Franco, G., Marechal, D., and Schröter, K.: A Review of Flood Loss Models as Basis for Harmonization and Benchmarking, PLOS ONE, 11, e0159 791, https://doi.org/10.1371/journal.pone.0159791, 2016.

Hua, P., Yang, W., Qi, X., Jiang, S., Xie, J., Gu, X., Li, H., Zhang, J., and Krebs, P.: Evaluating the effect of urban flooding reduction strategies in response to design rainfall and low impact development, Journal of cleaner production, 242, 118 515, 2020.

Knoche, F., Schumacher, F., Zamzow, M., Sohrt, J., Rehfeld-Klein, M., Matzinger, A., Johne, U., Meier, I., Rouault, P., and Pawlowsky-Reusing, E Schütz, P.: Strategic planning of blue-green infrastructure to reduce surface water pollution from combined sewer overflows, in: Extended abstracts, 2024.

Kottek, M., Grieser, J., Beck, C., Rudolf, B., and Rubel, F.: World map of the Köppen-Geiger climate classification updated, Meteorologische Zeitschrift, 2006.

LAWA: LAWA Starkregenportal, https://lawa-starkregenportal.okeanos.ai/, accessed: 2025-10-09, 2025.

Locatelli, L., Guerrero, M., Russo, B., Martínez-Gomariz, E., Sunyer, D., and Martínez, M.: Socio-economic assessment of green infrastructure for climate change adaptation in the context of urban drainage planning, Sustainability, 12, 3792, 2020.

LUBW: Anhänge 1 a, b, c zum Leitfaden Kommunales Starkregenrisikomanagement in Baden-Württemberg, 2020.

Mishra, S. K. and Singh, V. P.: Soil conservation service curve number (SCS-CN) methodology, vol. 42, Springer Science & Business Media, 2003.

Mohor, G. S., Thieken, A. H., and Korup, O.: Residential flood loss estimated from Bayesian multilevel models, Natural Hazards and Earth System Sciences, 21, 1599–1614, https://doi.org/10.5194/nhess-21-1599-2021, 2021.

Monberg, R. J., Howe, A. G., Ravn, H. P., and Jensen, M. B.: Exploring structural habitat heterogeneity in sustainable urban drainage systems (SUDS) for urban biodiversity support, Urban Ecosystems, 21, 1159–1170, 2018.

Montalvo, C., Reyes-Silva, J., Sañudo, E., Cea, L., and Puertas, J.: Urban pluvial flood modelling in the absence of sewer drainage network data: A physics-based approach, Journal of Hydrology, 634, 131 043, 2024.

Neumann, J., Scheid, C., and Dittmer, U.: Potential of decentral nature-based solutions for mitigation of pluvial floods in urban areas—A simulation study based on 1D/2D coupled modeling, Water, 16, 811, 2024.

OpenStreetMap contributors: OpenStreetMap, https://www.openstreetmap.org, 2024.

https://doi.org/10.5194/egusphere-2025-5466
Preprint. Discussion started: 21 November 2025

ORNL DAAC: Global Hydrologic Soil Groups (HYSOGs250m) for Curve Number-Based Runoff Modeling, https://daac.ornl.gov/SOILS/guides/Global_Hydrologic_Soil_Group.html, accessed: 2024-10-01, 2024.

Owolabi, T. A., Mohandes, S. R., and Zayed, T.: Investigating the impact of sewer overflow on the environment: A comprehensive literature review paper, Journal of Environmental Management, 301, 113 810, 2022.

Paprotny, D., Kreibich, H., Morales-Nápoles, O., Wagenaar, D., Castellarin, A., Carisi, F., Bertin, X., Merz, B., and Schröter, K.: A probabilistic approach to estimating residential losses from different flood types, Natural Hazards, 105, 2569–2601, 2021.

Peng, Z., Jinyan, K., Wenbin, P., Xin, Z., and Yuanbin, C.: Effects of Low-Impact Development on Urban Rainfall Runoff under Different Rainfall Characteristics., Polish Journal of Environmental Studies, 28, 2019.

Riechel, M.: Auswirkungen von Mischwassereinleitungen auf die Berliner Stadtspree, Tech. rep., Kompetenzzentrum Wasser Berlin gGmbH, https://publications.kompetenz-wasser.de/pdf/Riechel-2009-309.pdf, 2009.

Riechel, M., Matzinger, A., Pawlowsky-Reusing, E., Sonnenberg, H., Uldack, M., Heinzmann, B., Caradot, N., von Seggern, D., and Rouault, P.: Impacts of combined sewer overflows on a large urban river–Understanding the effect of different management strategies, Water research, 105, 264–273, 2016.

Riechel, M., Matzinger, A., Pallasch, M., Joswig, K., Pawlowsky-Reusing, E., Hinkelmann, R., and Rouault, P.: Sustainable urban drainage systems in established city developments: Modelling the potential for CSO reduction and river impact mitigation, Journal of Environmental Management, 274, 111 207, 2020.

Rossman, L. A. et al.: Storm water management model user's manual, version 5.0, National Risk Management Research Laboratory, Office of Research and . . . , 2010.

Samprogna Mohor, G., Lindenlaub, S., and Thieken, A.: Fast and operational building damage estimation tool for urban pluvial flooding, in: EGU General Assembly 2025, pp. EGU25–10 095, Vienna, Austria, 27 Apr–2 May 2025, https://doi.org/10.5194/egusphere-egu25-10095, 2025.

Schlea, D., Martin, J. F., Ward, A. D., Brown, L. C., and Suter, S. A.: Performance and water table responses of retrofit rain gardens, Journal of Hydrologic Engineering, 19, 05014 002, 2014.

Sieker, H. and Neidhart, N.: Planungshilfe für eine dezentrale Straßenentwässerung, 2018.

Staccione, A., Essenfelder, A. H., Bagli, S., and Mysiak, J.: Connected urban green spaces for pluvial flood risk reduction in the Metropolitan area of Milan, Sustainable Cities and Society, 104, 105 288, 2024.

Steffen, L. and Hinkelmann, R.: hms++: Open-source shallow water flow model with focus on investigating computational performance, SoftwareX, 22, 101 397, https://doi.org/https://doi.org/10.1016/j.softx.2023.101397, 2023.

Thieken, A., Kreibich, H., Müller, M., and Lamond, J.: Data collection for a better understanding of what causes flood damage – experiences with telephone surveys, in: Flood damage survey and assessment: new insights from research and practice, edited by Molinari, D., Menoni, S., and Ballio, F., chap. 7, pp. 95–106, AGU, Wiley, https://doi.org/10.1002/9781119217930.ch7, 2017.

Thieken, A. H., Müller, M., Kreibich, H., and Merz, B.: Flood damage and influencing factors: New insights from the August 2002 flood in Germany, Water Resources Research, 41, W12 430, https://doi.org/10.1029/2005WR004177, 2005.

Tügel, F., Nissen, K. M., Steffen, L., Zhang, Y., Ulbrich, U., and Hinkelmann, R.: Extreme precipitation and flooding in Berlin under climate change and effects of selected grey and blue-green measures, EGUsphere, 2025, 1–26, https://doi.org/10.5194/egusphere-2025-445, 2025.

Watrin, V. d. R., Blanco, C. J. C., and Gonçalves, E. D.: Thermal and hydrological performance of extensive green roofs in Amazon climate, Brazil, in: Proceedings of the Institution of Civil Engineers-Engineering Sustainability, vol. 173, pp. 125–134, Thomas Telford Ltd, 2019.

https://doi.org/10.5194/egusphere-2025-5466
Preprint. Discussion started: 21 November 2025

Weyrauch, P., Matzinger, A., Pawlowsky-Reusing, E., Plume, S., von Seggern, D., Heinzmann, B., Schroeder, K., and Rouault, P.: Contribution of combined sewer overflows to trace contaminant loads in urban streams, Water Research, 44, 4451–4462, 2010.

Zhang, L., Ye, Z., and Shibata, S.: Assessment of rain garden effects for the management of urban storm runoff in Japan, Sustainability, 12, 9982, 2020.